T2R2 東京工業大学リサーチリポジトリ
Tokyo Tech Research Repository

論文 / 著書情報
Article / Book Information

Title	Alternating pressure control system for hydraulic robots
Authors	Sarin Kittisares, Yosiharu Hirota, Hiroyuki Nabae, Gen Endo, Koichi Suzumori
Citation	Mechatronics, Volume 85, ,
Pub. date	2022, 5

Powered by T2R2 (Tokyo Institute Research Repository)

Mechatronics 85 (2022) 102822

Contents lists available at ScienceDirect

Mechatronics

journal homepage: www.elsevier.com/locate/mechatronics

Alternating pressure control system for hydraulic robots☆

Sarin Kittisares *, Yosiharu Hirota, Hiroyuki Nabae, Gen Endo, Koichi Suzumori

Department of Mechanical Engineering, Tokyo Institute of Technology, 2 Chome-12-1 Ookayama, Meguro, 152-8550, Tokyo, Japan

ARTICLE INFO

Keywords:
Hydraulics
Robotics
Alternating pressure

ABSTRACT

Hydraulics is a promising technology for robots. However, traditional hydraulic infrastructures are often large and power-inefficient, with large power sources that hinder mobility. In contrast, electro-hydrostatic actuators are relatively power efficient, but their cost and weight can be excessive in systems with a higher number of degrees of freedom. In this paper, we propose a new alternating pressure control system for hydraulic systems with a higher number of degrees of freedom based on an alternating pressure source system. In this system, the valves open and close in synchronization with a pump with sensor feedback, allowing either pressure or position in each actuator to be controlled independently. With the proposed system, a centralized pump can be used with simplified tubing and simple on–off valves. Moreover, we developed a dynamic duty ratio system that improves performance and reduces pump utilization time. The experimental results confirmed that both the position and pressure of each actuator can be controlled in parallel on a multi-degree-of-freedom system.

1. Introduction

Hydraulic actuators have been employed in heavy machinery for a long time owing to their large force output, high force and power density, and good impact resistance. These advantages make them suitable for tough robotic applications [1–4], mobile robots [5–8], and wearable robots [9,10]. Hydraulic actuators also have a potential to be adopted in other multi-degree-of-freedom mechanical systems, which are also considered as robots in the context of this paper. In addition, soft hydraulic actuators that often operate using fluid power are utilized for applications such as hydraulic artificial muscles. In our earlier work, we developed a sit-to-stand support device based on hydraulic artificial muscles [11]. While the device had a satisfactory force output, the hydraulic supply system and its power consumption remained a challenge. In mobile robots and wearable robots, reduced power consumption will improve operational range and duration, which are crucial in actual application.

Traditional hydraulic infrastructure consists of a centralized pump and tank, and the hydraulic pressure is delivered to the actuators through piping. The supply pressure is controlled via a pressure relief valve, and the actuators are controlled with flow control valves or pressure control valves. However, it has been mentioned in the literature that in conventional valve-controlled hydraulic systems, where hydraulic pressure is supplied from a central hydraulic unit and controlled through a valve, the hydraulic unit runs continuously, even when not active, leading to a lower efficiency [10,12–14].

In contrast, the electro-hydrostatic actuator (EHA) only needs to be powered when actuated, leading to a higher power efficiency compared to traditional systems [10,12–14]. Originally developed for applications in aircrafts, the EHA combines electrical motors, pumps, accumulators, valves, hydraulic actuators, and electrical circuits into a single unit. The EHA is a pump-controlled system, and pressurized fluid is only used for transmission between the motor and actuator. In robotic applications, EHAs are often utilized when smaller sizes and weight-to-power ratios are essential, such as in prostheses or exoskeletons [9,14].

In systems with a higher number of degrees of freedom, all EHAs operate in parallel with each other. This is an advantage for aircraft applications when each actuator is positioned in a different part of the aircraft since piping from a centralized supply unit is then eliminated [12,13]. On the other hand, in robots, where actuators are positioned close to each other, the weight of the piping is negligible. However, the redundant hydraulic components of each EHA, particularly pumps and motors, result in an excessive cost and weight of the entire system.

Another alternative to the conventional centralized hydraulic system is the alternating pressure source with a synchronized valve system, which has been previously proposed for microactuators [15,16]. In this system, an alternating pressure is supplied to all actuators simultaneously. Control valves, which are directly connected to the actuators, open and close in synchronization with the pump. For example, to elongate the actuator, the valve opens during the pressurized period and closes during the suction period.

☆ This paper was recommended for publication by Associate Editor Gianluca Palli.

* Corresponding author.
E-mail address: kittisares.s.aa@m.titech.ac.jp (S. Kittisares).

https://doi.org/10.1016/j.mechatronics.2022.102822
Received 2 August 2021; Received in revised form 5 March 2022; Accepted 2 May 2022
Available online 18 May 2022
0957-4158/© 2022 The Author(s). Published by Elsevier Ltd. This is an open access article under the CC BY license (http://creativecommons.org/licenses/by/4.0/).

With the alternating pressure system, the piping is simplified and only a simple on–off valve is required, rather than the complex 3/3 flow control valve required to achieve the same functionality as the traditional single-acting cylinder system. In both studies, an electro-rheological fluid, controlled with flexible electro-rheological microvalves, was utilized as the hydraulic fluid. They achieved independent motion of the two actuators. However, as the system was designed for a microactuator, its functionality as a hydraulic supply system is very limited: neither pressure nor volume can be controlled, and the input peak-to-peak pressure is only 110 kPa. Lastly, the pump in this system also needs to run continuously, resulting in low power efficiency.

Another important component of hydraulic systems is hydraulic fluid. While oil-based hydraulic liquids are often used in traditional systems, water-based hydraulic liquids have also been proposed as alternatives because they are more user-friendly, accessible, and environmentally friendly [17,18]. These advantages make water an appealing choice for wearable devices that are in close contact with the user.

In this paper, we propose a new alternating pressure control system (APCS) based on an alternating pressure source system, wherein each hydraulic actuator is connected to a centralized alternating pressure source and an on–off valve. However, instead of simply synchronizing the valves to the pump in an open-looped fashion, the pressure and position sensors allow a more complex algorithm to be utilized, thereby improving functionality. We propose a control algorithm utilizing on–off valves, feedback signals, and an alternating pressure source in a multi-degree-of-freedom system. In the proposed system, the pressure in each actuator is "updated" at a semi-fixed period, allowing both pressure and volume in each actuator to be controlled simultaneously. Furthermore, we also propose a dynamic duty ratio algorithm to reduce total pump utilization time and improve power consumption. The performance and effectiveness of the proposed system are validated through simulations and experiments. The APCS reduces the weight and cost of EHAs while enabling lower power consumption and requiring fewer components than conventional centralized systems. We believe this system will be beneficial multi-degree-of-freedom systems where high power efficiency is needed, such as mobile robots.

2. Proposal of the alternating pressure control system

A general APCS consists of one centralized servo pump and one on–off valve per actuator, similar to the alternating pressure source system. However, in APCS, pressure sensors or position sensors can also be installed for feedback according to the desired operating mode, as shown in Fig. 1. The inclusion of feedback sensors allows the controller to control either pressure or position of each actuator, as well as stop the motor when not required to reduce power consumption.

The control algorithm of APCS can be described as follows. First, the controller compares the setpoint and output of the system and determines the operating mode required. If all actuators are at the setpoint, the valves are closed, and the motor stops. However, if the pressure or volume in one or more actuators needs to be increased or decreased, the motor turns forward or backward, respectively. Simultaneously, the valves at the corresponding actuator open, allowing the motor to power the actuator as a motor-controlled hydraulic system. If the pressure or volume in certain actuators must be increased and decreased simultaneously, then the motor applies alternating pressure to the system. Subsequently, the controller compares the supply and actuator pressures, and then opens or closes the valve according to the algorithm. In addition, a dynamic duty ratio was employed to maintain a balanced performance between all the actuators during the alternating pressure mode, i.e., the APCS operates as a hybrid of a pump-controlled system and a valve-controlled system.

The system in this study consists of one positive displacement pump powered by a servo motor, four double-acting cylinders operating as single-acting cylinders, four on–off valves, and five pressure sensors,

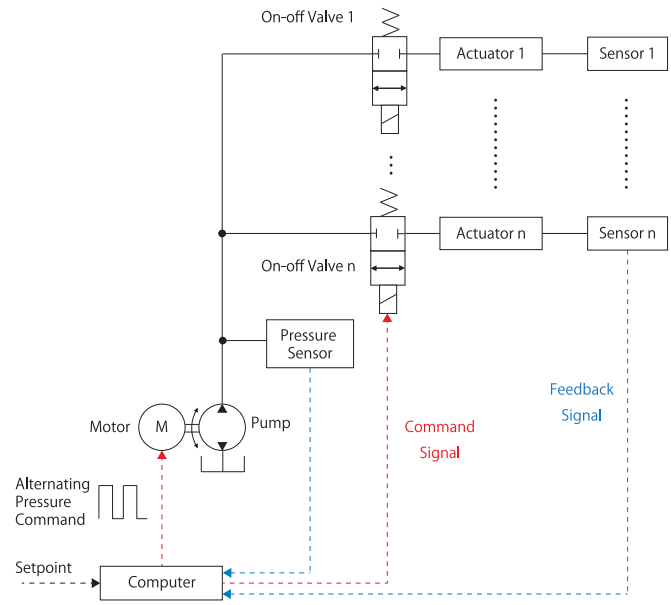

Fig. 1. Outline of the proposed system, consisting of a motor, a pump, and a theoretically unlimited number of sets of on–off valves and actuators. The on/off valves open and close in sync with the alternating pressure from the pump.

with water as the hydraulic fluid. The pump operated in a pressure-controlled mode and had a maximum operating pressure of 5 MPa. To utilize the double-acting cylinder as a single-acting cylinder, the hydraulic pressure is only connected to one side of the cylinder, while a constant pneumatic pressure is applied to the other side as a return mechanism. Further, instead of simply synchronizing the valves to the alternating pressure in an open-looped fashion, pressure sensors and linear potentiometers were installed for feedback, which allows a more complex control algorithm to be utilized for pressure and position control.

2.1. Alternating pressure source

The alternating pressure source is an integral part of this study. Higher frequencies result in quicker system response and less delay; however, this response is restricted by the limitations of the pump and servo motor and the operating speed of the valve. Moreover, different alternating pressure waveforms can also lead to variable performance depending on the type of application. An APCS with a rectangular wave, associated with abrupt changes of pressure in the alternating pressure source, would enable a faster response with a higher alternating frequency. This makes a rectangular wave source pressure suitable if the actuator only requires the pressure to be on or off. In contrast, a sinusoidal wave alternating pressure source exhibited a more gradual change in pressure. This allows the valves to open or close at any point between the maximum and minimum pressures and additionally allows any pressure value between the minimum and maximum values to be used as a setpoint.

For a rectangular wave, it is also possible to manipulate the duty ratio to improve the overall performance of all the cylinders. Herein, the dynamic duty ratio function for a system with n actuators is expressed as Eq. (1)

$$\mathrm{DR} = \frac{1}{2}\left(\frac{\sum_{i=1}^{n} \mathrm{sgn}(x_{r,i} - x_i)}{\sum_{i=1}^{n} |\,\mathrm{sgn}(x_{r,i} - x_i)|} + 1\right). \tag{1}$$

where

i is the number of the actuator;

$x_{r,i}$ is the setpoint of actuator i for the relevant mode (force or displacement); and

x_i is the current output of actuator i.

Function sgn denotes the signum function, which is defined as follows:

$$\mathrm{sgn}(x) := \begin{cases} -1 & \text{if } x < 0, \\ 0 & \text{if } x = 0, \\ 1 & \text{if } x > 0. \end{cases} \tag{2}$$

However, a duty ratio value that is too low results in a short pulse, which does not provide sufficient time for the pump to reach the desired value. Similarly, a very high duty ratio value results in the pressure not falling to the desired value. To prevent this, the rise time (t_{rise}), fall time (t_{fall}), and alternating pressure frequency (f) of the pump can be used to calculate the applicable range of the dynamic duty ratio value, as shown in the equation below:

$$DR_{\text{applicable}} = \begin{cases} 0 & \text{if } DR = 0, \\ t_{\text{rise}} f & \text{if } 0 < DR \le t_{\text{rise}} f, \\ DR & \text{if } t_{\text{rise}} f < DR < 1 - t_{\text{fall}} f \\ 1 - t_{\text{fall}} f & \text{if } 1 - t_{\text{fall}} f \le DR < 1 \\ 1 & \text{if } DR = 1. \end{cases} \tag{3}$$

The value of t_{rise} and t_{fall} in the context of this paper are obtained experimentally as the time taken by the pump to reach maximum pressure or minimum pressure after receiving a step input signal.

While only the rectangular wave and the sinusoidal wave were used in this study, other waveforms such as sawtooth or triangular waves, which also have gradual pressure changes, can also be considered in a future study.

2.2. Valve controller

2.2.1. Pressure control

The valve controllers compare the source pressure, the pressure inside the actuators, and setpoint, and then open or close the valves depending on the situation. The basic logic of the valve controller is given by Eq. (4). The logical operator AND and OR are denoted as $\wedge$ and $\vee$ respectively.

$$((P_s > P_a) \wedge (P_r > P_a)) \vee ((P_s < P_a) \wedge (P_r < P_a)) \implies V_{\text{open}}. \tag{4}$$

where

P_s is the source pressure;

P_r is the reference pressure; and

P_a is the actuator pressure.

Moreover, to prevent overshoot, which would increase the error instead of reducing it, the valve should only open when P_r is closer to P_s than to P_a, i.e.,

$$|P_r - P_s| < |P_r - P_a|. \tag{5}$$

The stability of the system can be improved by using a dead zone around the target pressure. The implementation of the valve controller in MATLAB Simulink is shown in Fig. 2

2.2.2. Position control

Operation in this mode is relatively simple: a rectangular wave with a dynamic duty ratio expressed in Eq. (1) is provided to the pump. The valve then opens or closes according to the direction of the pump and the desired cylinder direction.

The dynamic duty ratio allows all the actuators to be equally prioritized while improving the performance when only a number of actuators are active.

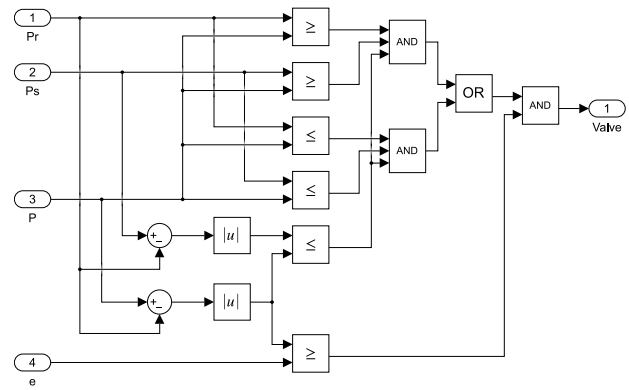

Fig. 2. Implementation of the valve controller logic in a pressure-controlled pump for a force-controlled mode in Simulink where e is the value of dead band.

Table 1
Parameters used in the simulation.

Parameter	Value
System temperature	293.15 K
Atmospheric pressure	0.101325 MPa
Pump rise time	0.1 s
Pump fall time	0.1 s
Cylinder piston diameter	20 mm
Cylinder piston stroke	0.2 m
Valve delay	20 ms
Valve orifice diameter	1.5 mm
Valve leakage area	1×10^{-10} m^2

3. Simulation

The system was simulated using MATLAB 2021a Simulink and Simscape software. The pumps in the pressure- and volume-controlled modes were modeled as perfect pressure sources. The transient response of the pump was modeled as an underdamped unity-gain second-order system with the transfer function shown in Eq. (6). Further, four sets of hydraulic cylinders and valves were connected to the pump. The components are modeled after the experimental equipment, which is explained in detail in Section 4.1. We assume that liquid temperature was constant and there was no deformation in the components. Other conditions including cylinder friction, valve leakage, fluid compressibility and viscosity, volume of tubing were already considered. The parameters in the simulations are obtained experimentally and are given in Table 1.

$$G(s) = \frac{100^2}{s^2 + 160s + 100^2} \tag{6}$$

3.1. Pressure control

In the pressure control mode, both rectangular and sinusoidal waves were used for the source pressure and setpoint. This results in four combinations:

1. Rectangular source, rectangular setpoint (R–R)
2. Sinusoidal source, rectangular setpoint (S–R)
3. Rectangular source, sinusoidal setpoint (R–S)
4. Sinusoidal source, sinusoidal setpoint (S–S).

The hydraulic cylinders in the pressure control mode were simulated to be fixed with no external force acting on the cylinder. The valves were simulated as gate valves with a transport delay of 50 ms to emulate the actuation time of the real valve. The models of the valve and cylinder are shown in Fig. 3.

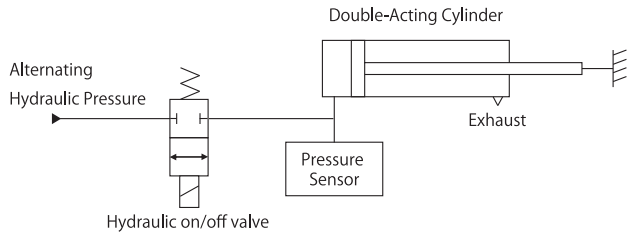

Fig. 3. The model of the valve and cylinder in pressure control mode simulations. The cylinder rod was fixed, and the volume within the cylinder was constant.

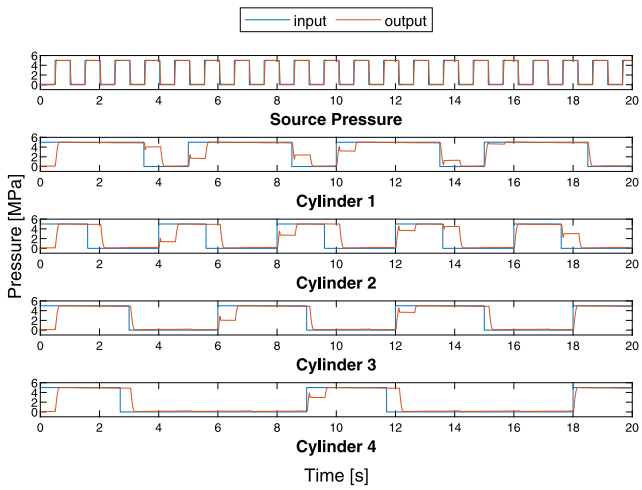

Fig. 4. Simulation results in the R-R mode with a 1 Hz source frequency and a 0.2 MPa deadband.

The performance of the simulated system is calculated using the root mean square error (RMSE) defined as shown in Eq. (7)

$$\mathrm{RMSE} = \sqrt{\frac{1}{n}\sum_{i=1}^{n}(P_{\mathrm{r},i} - P_i)^2}. \tag{7}$$

where:

n is the number of sampled points;

$P_{r,i}$ reference pressure; and

P_i is the cylinder pressure.

In addition, for sinusoidal setpoint modes, the output delay was also calculated. A discrete Fourier transform is used to obtain the phase difference between the setpoint and pressure output, which is then used to calculate the time delay. The theoretical maximum delay corresponds to the period of the alternating pressure.

The setpoints in the rectangular setpoint modes were rectangular waves with different frequencies and pulse widths. The APCS could control the pressures in all cylinders simultaneously with both rectangular and sinusoidal pressure sources, as shown in Figs. 4 and 5. The sinusoidal pressure source has a more gradual change in pressure, resulting in a larger delay compared with the rectangular pressure source mode. However, all delays were less than the period of the alternating pressure source. Further, the RMSE values for the R-R and S-R modes were 1.21 and 1.56 MPa, respectively.

The application of the dynamic duty ratio reduces the total pump utilization time in the R-R mode from 50% to 41.22% and increases the RMSE to 1.62 MPa. The dynamic duty ratio decreases energy consumption by reducing the pump utilization time when all actuators are already in place; in addition, it improves the performance by increasing the pump utilization time when activating an actuator. However, the improved performance was not apparent in this simulation, where all cylinders were at a fully extended position with a virtually fixed volume. The current implementation of the dynamic duty ratio increases the theoretical maximum delay to two periods of the source pressure, which also results in an increased RMSE. The simulation results are shown in Fig. 6.

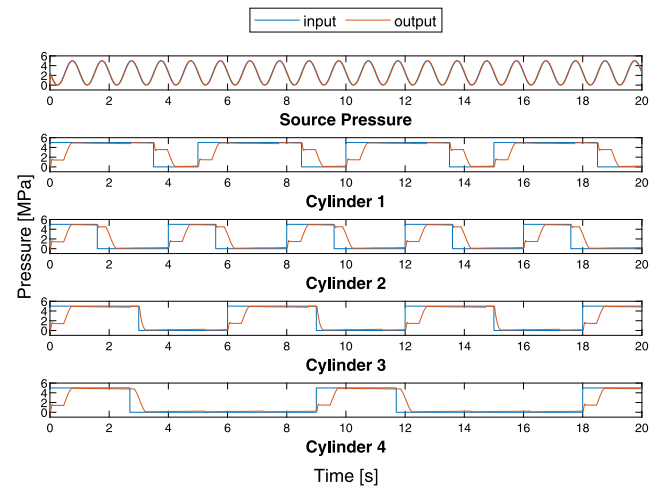

Fig. 5. Simulation results in the S-R mode with a 1 Hz source frequency and a 0.2 MPa deadband.

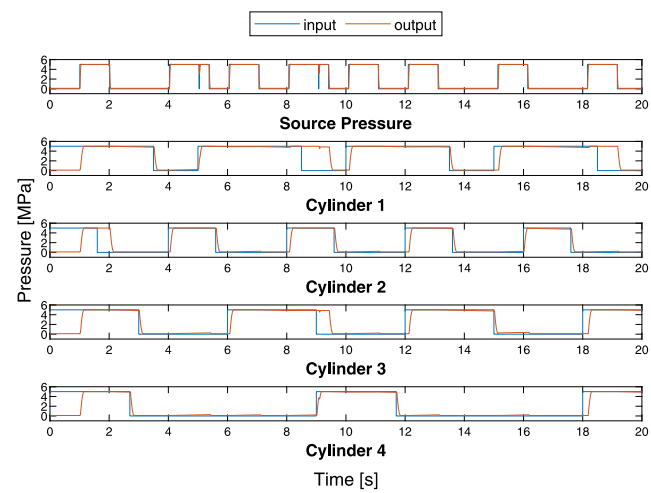

Fig. 6. Simulation results in the R-R mode with dynamic duty ratio with a 1 Hz source frequency and a 0.2 MPa deadband.

Table 2
RMSE and delay in S-S mode from 1 Hz to 5 Hz. The dead band was 0.2 MPa.

Frequency (Hz)	1	2	3	4	5
RMSE (MPa)	0.69	0.52	0.41	0.40	0.46
Delay (s)	0.30	0.16	0.13	0.10	0.10

Simulations with sinusoid setpoint modes yielded contrary results; using a sinusoid wave as the source pressure resulted in lower delay and error, as shown in Figs. 7 and 8. This is because sinusoidal waves have a more gradual change in pressure compared to rectangular waves, which allows the valves more time to shut at the reference pressure. As a result, the R-S mode has a larger delay (0.61 s) and RMSE (1.22 MPa) compared to the corresponding values for the S-S mode (0.30 s, 0.69 MPa).

Increasing the source pressure frequency improves both the RMSE and the delay of the system. The delays and RMSEs of the S-S mode between the 1 and 5 Hz source frequencies are shown in Table 2.

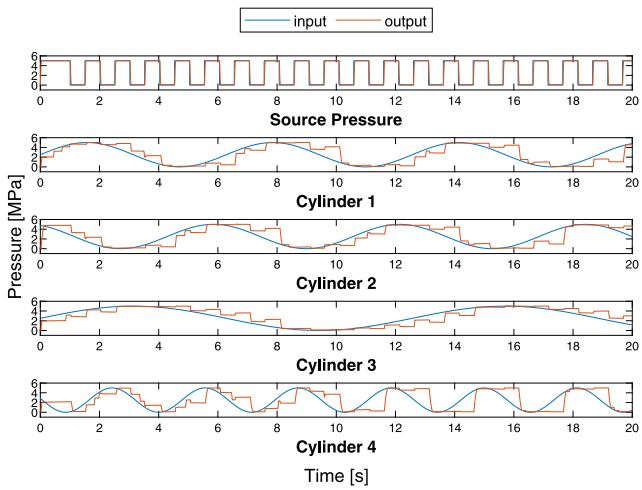

Fig. 7. Simulation results in the R-S mode with a 1 Hz source frequency and a 0.2 MPa deadband.

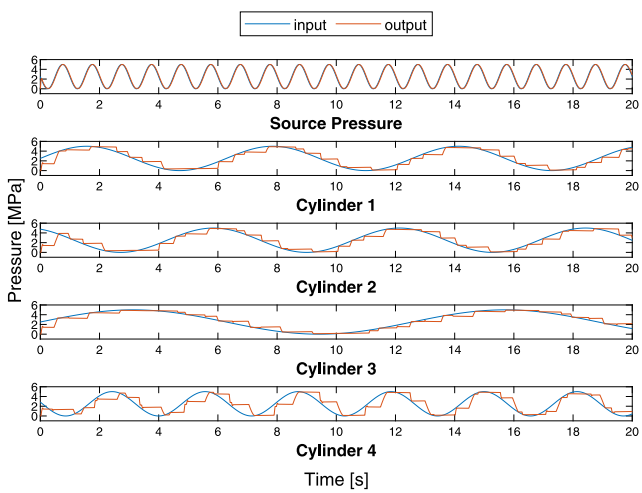

Fig. 8. Simulation results in the S-S mode with a 1 Hz source frequency and a 0.2 MPa deadband.

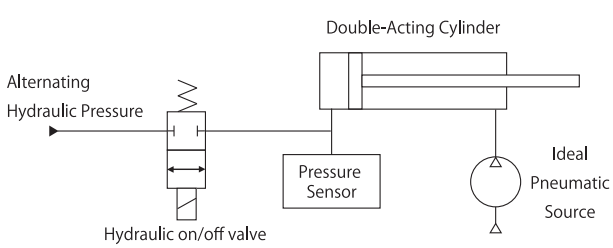

Fig. 9. The model of the valve and cylinder in the position control mode simulations. The double-acting cylinder acts as a single-acting cylinder with a constant pressure as the return mechanism.

3.2. Position control

In the position control mode, a constant pneumatic pressure of 0.9 MPa is applied to the cylinder as a return mechanism instead of a return spring. This was simulated as a constant force of an equivalent magnitude acting on the rod. Further, the valves were simulated as gate valves with a transport delay of 50 ms, similar to the pressure control mode. The models of the valve and cylinder are shown in Fig. 9.

The simulated system could operate all four hydraulic cylinders independently. The resulting positions of the hydraulic cylinder rods

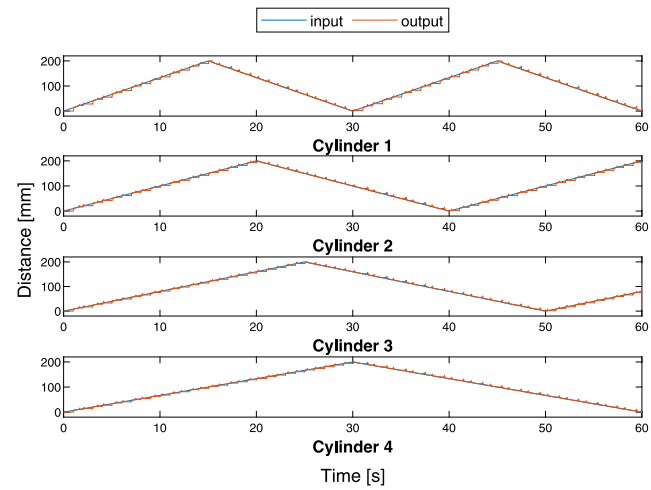

Fig. 10. The model of the valve and cylinder in the position control mode in Simulink Simscape.

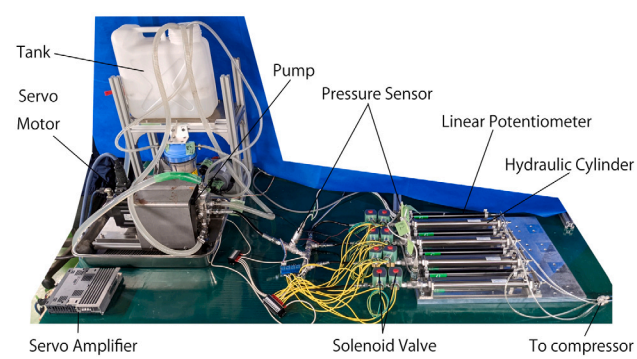

Fig. 11. Experiment setup. The controller box and compressor are not shown in this figure.

with a 5 mm dead band are shown in Fig. 10. The RMSE of all four cylinders is 3.17 mm. The pump was activated for a total of 16.30 s, which is 32.60% of the operating time.

While setting the dead band to 0 mm offers a very slight reduction of RMSE to 3.10 mm, it increases the pump utilization time by 75% to 28.14 s or 56.28% of the operating time. In contrast, increasing the dead band to 10 mm increases the RMSE to 5.05 mm and reduces the pump utilization time to 11.63 s, or 23.26% of the operating time.

4. Experiments

4.1. Experiment setup

The experimental setup consisted of a water pump (ASP035-T110, LEVEX Corporation, Kyoto, Japan) connected to a 3-phase servo motor (HG-SR51B, Mitsubishi Electric Corporation, Tokyo, Japan). The servo motor was powered by a servo amplifier (MR-J4a, Mitsubishi Electric Corporation, Tokyo, Japan) and connected to a controller board (MicroLabBox, dSPACE Inc., MI, USA) operating at 1 kHz. Further, two solenoid flow control valves (HTJ262G002, ASCO Japan Co. Ltd., Hyogo, Japan) were connected in opposite directions to operate as a single on/off valve. The double-acting hydraulic cylinders (KS-5LB20 × 20, JPN Co. Ltd., Tokyo, Japan) have an inner diameter of 20 mm and a stroke of 200 mm. In addition, the pressures were measured using pressure sensors (PSE577, SMC Corporation, Tokyo, Japan). The constant air pressure of 0.9 MPa, which acts as a return mechanism in the position-controlled modes, was regulated with a

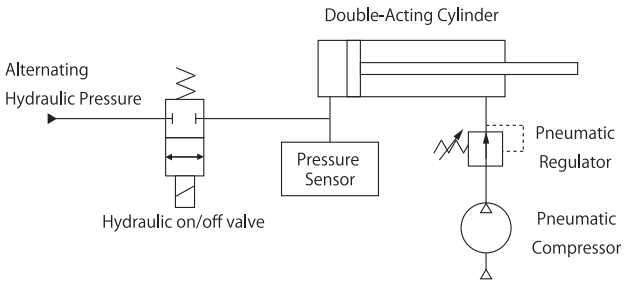

Fig. 12. Schematic of the experiment setup.

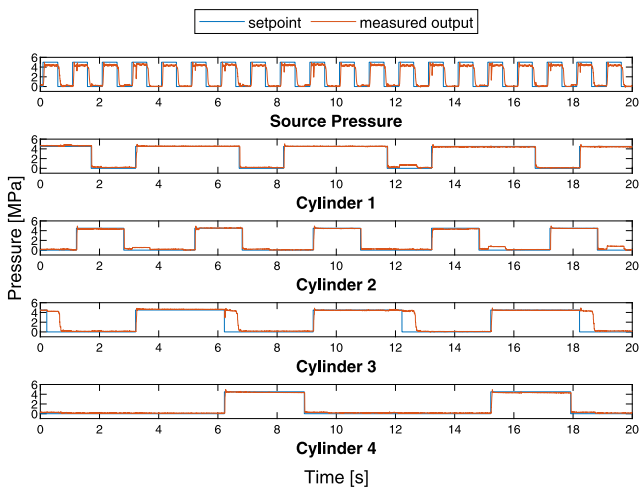

Fig. 13. Experiment results in the R-R mode with a 1 Hz source frequency and a 0.2 MPa deadband. This is an example of a suitable configuration.

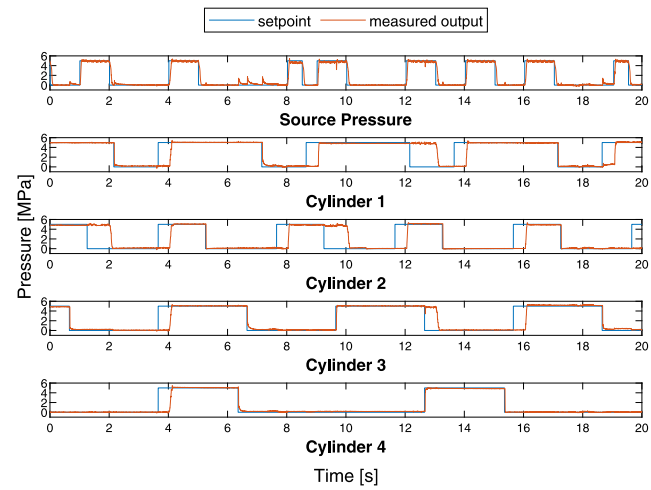

Fig. 14. Experiment results in the R-R mode including the dynamic duty ratio, with a 1 Hz source frequency and a 0.2 MPa deadband. The dynamic duty ratio reduces the pump utilization.

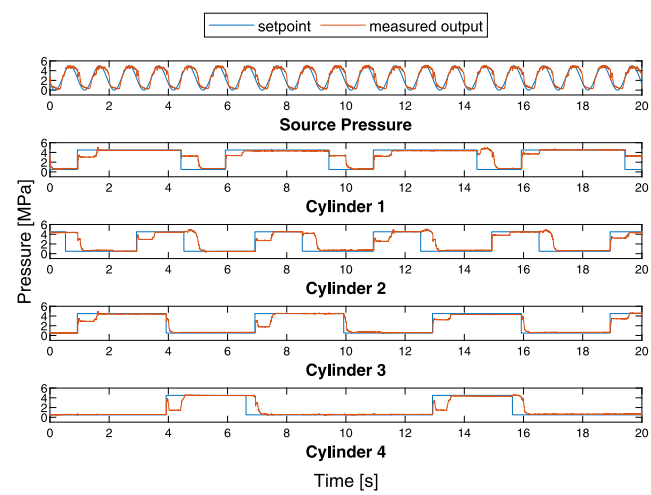

Fig. 15. Experiment results in the S-R mode with a 1 Hz source frequency and a 0.2 MPa deadband. This is an unsuitable configuration because sinusoidal source pressure has a slower pressure change, resulting in a larger error.

filter regulator (FRF300-02-MD, Nihon Pisco Co. Ltd., Nagano, Japan) and a positive pressure sensor (GPD-01, Nihon Pisco Co. Ltd., Nagano, Japan). In the experiments in a loaded condition, the external load was simulated with a pneumatic pressure regulated by an electro pneumatic regulator (MEVT500-0C4-T11R-4U3, CKD Corporation, Aichi, Japan). In total, 5 pressure sensors, 4 linear potentiometers, and 8 solenoid valves were used. The experimental setup is illustrated in Fig. 11, and the schematic of each actuator is shown in Fig. 12.

4.2. Pressure control

In the pressure control mode, all cylinders are in a fully-extended position, and the pneumatic pressure was set to 0 MPa.

4.2.1. Rectangular setpoint

The experimental results at 1 Hz source pressure frequency were consistent with the simulation results. In the R-R mode with a constant duty ratio of 0.5, the RMSE was 0.61 MPa, which was lower than the simulated result of 1.21 MPa (see Fig. 13).

Applying the dynamic duty ratio to the alternating pressure source reduced the total pump utilization time to 40.78% and increased the RMSE to 1.55 MPa. The increase in RMSE was due to the controller prioritizing the activation or deactivation of the actuator. For example, the error in Cylinder 1 in Fig. 14 between 12 and 13 s was due to the controller prioritizing the activation of cylinder 2 before updating the dynamic duty ratio at the 13 s mark. While this results in a larger error in this experimental setup where the cylinders are fixed, the dynamic duty ratio may improve performance in situations where cylinder rod movement is required.

In the S-R mode, the RMSE was 1.13 MPa, which was lower than 1.56 MPa in the simulations. For the rectangular setpoint modes, the sinusoidal source pressure offers a larger error and slower response compared to the rectangular source pressure. Furthermore, utilization of the dynamic duty ratio is not possible with a sinusoidal source pressure (see Fig. 15).

To demonstrate the performance of the APCS at a higher source frequency, experiments were also conducted between 1 Hz and 5 Hz. Increasing the source frequency to 5 Hz reduced the delay significantly as shown in Fig. 16. The RMSE at 5 Hz source frequency was 0.65 MPa.

Applying the dynamic duty ratio at a higher source frequency results in a significantly reduced pump utilization time to 21.96% at 3 Hz and 22.50% at 5 Hz source frequency as shown in Fig. 17. Moreover, the RMSE was also substantially reduced to 0.66 MPa. Utilizing the dynamic duty ratio at a higher source frequency results in a significantly reduced pump utilization time with an insignificant impact on RMSE. The pump utilization percentage at different source frequencies is summarized in Table 3.

4.2.2. Sinusoidal setpoint

Operation in the R-S mode also returned a similar result for the simulation. The valves could not react to the sudden pressure change, resulting in a larger error compared to the S-S mode. The delay and

Table 3
Pump utilization time at different source frequency with the dynamic duty ratio.

Frequency (Hz)	1	2	3	4	5
Pump utilization (%)	40.78	28.62	21.96	21.89	22.50

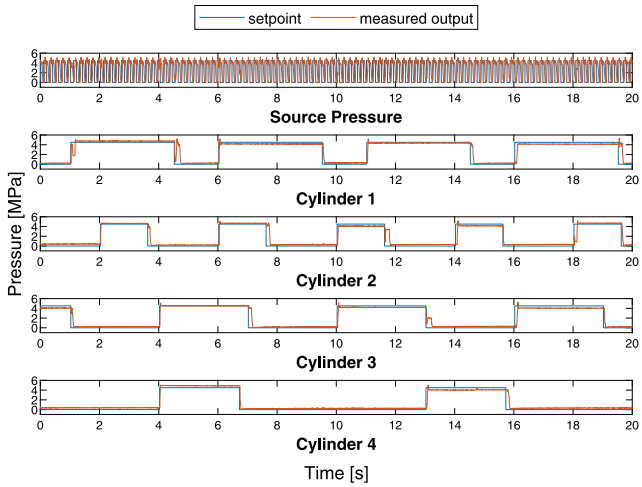

Fig. 16. Experiment results in the R-R mode with a 5 Hz source frequency and a 0.5 MPa deadband.

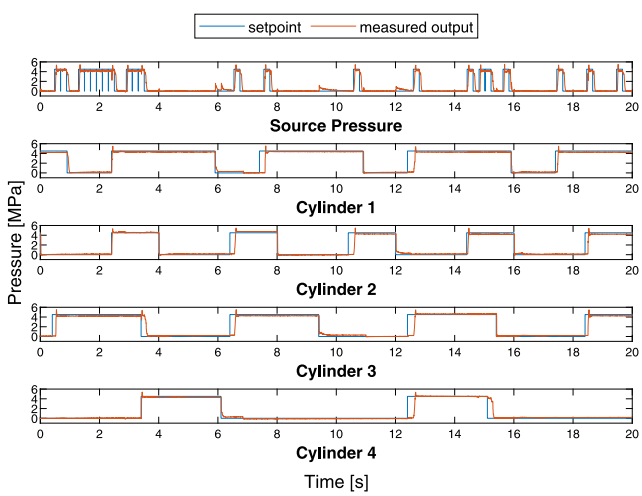

Fig. 17. Experiment results in the R-R mode dynamic duty ratio with a 5 Hz source frequency and a 0.2 MPa deadband.

RMSE in the R-S mode for an alternating source frequency of 1 Hz and a 0.2 MPa dead band were 0.29 s and 1.17 MPa, respectively.

Finally, in the S-S mode with a frequency of 1 Hz and a 0.2 MPa dead band, the average RMSE and delay were 0.64 MPa and 0.32 s, respectively, as shown in Fig. 19. This is similar to the corresponding simulation results of 0.69 MPa and 0.30 s, respectively.

Similar to the simulations, increasing the source frequency reduced the delay. Unlike the simulation, however, the RMSE increased at a higher frequency. We believe this was caused by the valves being slower in the experiments, resulting in a larger "overshoot" error, as shown in Fig. 20. Moreover, the RMSE value also depends on the frequency of the setpoint signal. The RMSE of Cylinder 3, which has the slowest setpoint frequency, is significantly lower than that of Cylinder 4 which has the fastest setpoint frequency within the same configurations. The RMSE and delay values between 1 and 5 Hz with a 0.2 MPa dead band are summarized in Table 4.

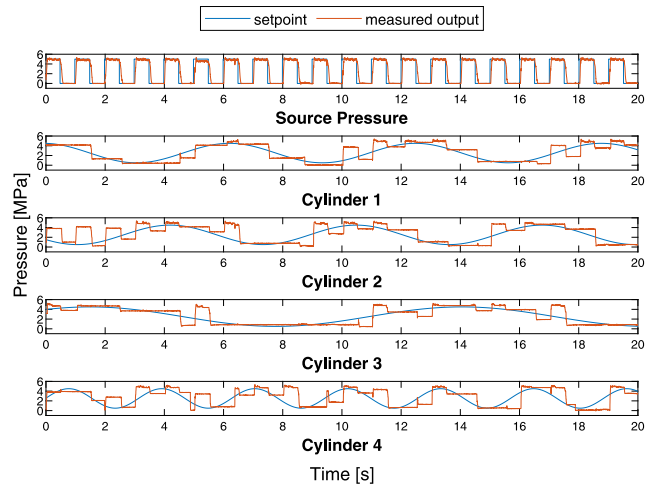

Fig. 18. Experiment results in the R-S mode with a 1 Hz source frequency and a 0.2 MPa deadband. Operation in this mode results in "overshoot" errors because the valves are not fast enough to close at the setpoint pressure. This is an example of an unsuitable configuration.

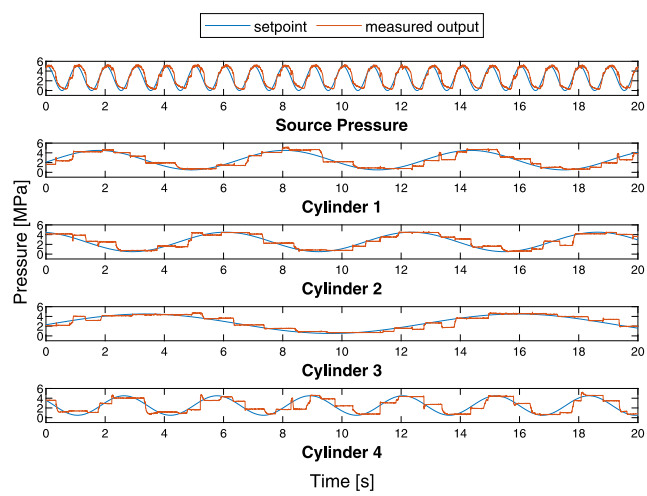

Fig. 19. Experiment results in the S-S mode with a 1 Hz source frequency and a 0.2 MPa deadband. This is an example of a suitable configuration.

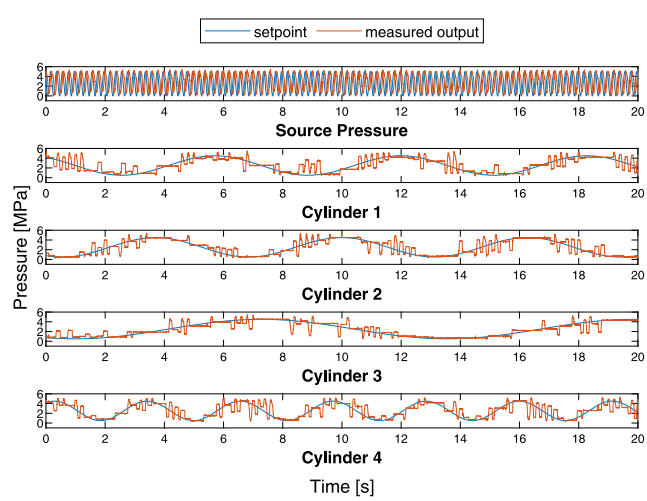

Fig. 20. Experiment results in the S-S mode with a 5 Hz source frequency and a 0.2 MPa deadband. The "overshoot errors" occurred due to the faster pressure change, similar to the R-S mode. This is another example of an unsuitable configuration.

Table 4
RMSE and delay in S-S mode from 1 Hz to 5 Hz. The dead band was 0.2 MPa.

Frequency (Hz)	1	2	3	4	5
Overall RMSE (MPa)	0.64	0.67	0.80	0.82	0.85
Cylinder 1 RMSE (MPa)	0.58	0.60	0.79	0.78	0.94
Cylinder 2 RMSE (MPa)	0.60	0.61	0.81	0.87	0.81
Cylinder 3 RMSE (MPa)	0.47	0.62	0.63	0.80	0.67
Cylinder 4 RMSE (MPa)	0.84	0.75	0.88	0.82	0.97
Overall delay (s)	0.32	0.17	0.14	0.11	0.13

Table 5
RMSE (mm) in position control mode at different alternating source frequencies and dead band values.

Dead Band (mm)	Frequency (Hz)		
	1	2	3
0	4.45	3.03	4.99
5	4.90	3.54	3.29
10	5.51	4.53	4.48

Table 6
Pump utilization time (%) in the position control mode at different alternating source frequencies and dead band values.

Dead Band (mm)	Frequency (Hz)		
	1	2	3
0	57.66%	55.82%	49.62%
5	47.81%	38.87%	34.51%
10	43.26%	25.72%	26.07%

Increasing the source frequency beyond 5 Hz was not possible with our current experimental equipment.

4.3. Position control

The experiment in the position control mode with a 5 mm dead band (see Fig. 21) also showed a similar result when compared to the simulations, with an RMSE of 4.90 mm, compared to the simulated value of 3.17 mm. Moreover, changing the frequency or dead band gap showed no significant reduction in error in the experiment, as shown in Table 5.

In contrast, increasing both the frequency and the dead band gap resulted in a substantial reduction in the pump utilization time. At a source frequency of 3 Hz and a dead band gap of 10 mm, the pump utilization time was reduced to 26.07% as shown in Table 6.

4.4. Load disturbance

In this section, we verify the performance of APCS with load disturbance in both the pressure control mode and position control mode.

4.4.1. Pressure control

In the pressure control mode, the external force acting on the cylinder in the return direction was simulated by applying air pressure to the hydraulic cylinder. For the constant loading experiment, a constant pneumatic pressure of 0.75 MPa was applied to the cylinder, which is the equivalent of 172.5 N. For the dynamic loading experiment, a sinusoidal pneumatic pressure with an amplitude of 0.25 MPa, bias of 0.25 MPa, and angular velocity of 1.5 πrad/s was applied to the cylinder to simulate an external force between 0 to 115 N acting on the rod. The source pressure frequency and dead band in this section are 1 Hz and 0.2 MPa, respectively.

Adding disturbance to the system result in a slight increase in RMSE, with a larger error with dynamic disturbance as shown in Table 7. The errors in R-R mode with disturbance are much higher than without disturbance but still lower than the simulated result without disturbance of 1.21 MPa. Experiment results in R-R mode with dynamic disturbance are shown in Fig. 22.

Table 7
RMSE (MPa) in pressure control mode with external disturbance.

Mode	Disturbance		
	None	Constant	Dynamic
R-R	0.61	1.02	1.18
S-R	1.13	1.17	1.27
R-S	1.17	1.22	1.33
S-S	0.64	0.86	0.80

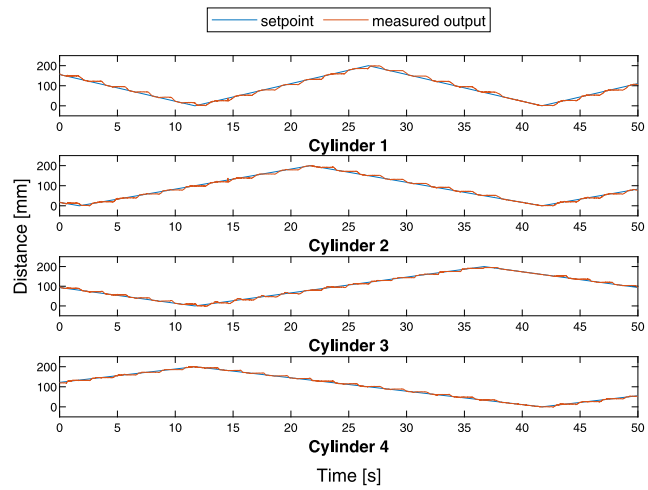

Fig. 21. Experiment results in the position control mode with a 1 Hz source frequency and 5 mm dead band.

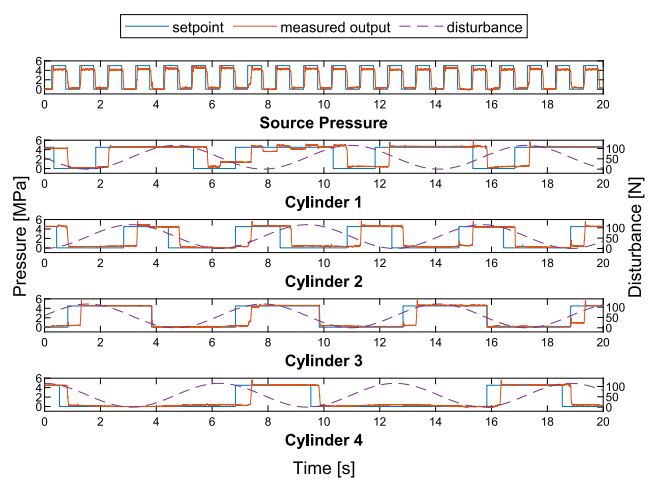

Fig. 22. Experiment results in the R-R mode with dynamic disturbances. The effects of disturbance can be seen most clearly in Cylinder 4.

4.4.2. Position control mode

In the position control mode, an external force acting on the rod in the extension direction was simulated by reducing the pneumatic pressure to a sine wave with an amplitude of 0.125 MPa, bias of 0.375 MPa, and angular velocity of 1.5 πrad/s. This is equivalent to an external force between 92 N to 149.5 N.

The error in position control mode increased due to the return mechanism having less force and thus became slower than without external force. The experiment results are shown in Fig. 23 and summarized in Table 8.

5. Discussion

In the pressure control mode, we proposed the APCS with two source pressure waveforms, namely a rectangular wave and a sinusoidal

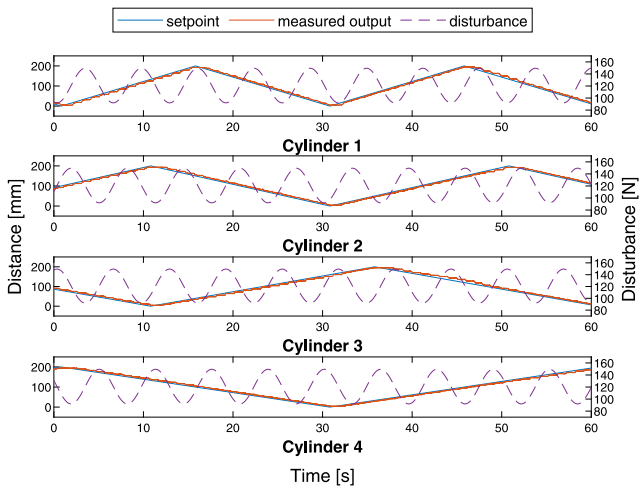

Fig. 23. Experiment results in the position control mode with a 1 Hz source frequency, 5 mm dead band and dynamic disturbances.

Table 8
RMSE (mm) in position control mode with external disturbance.

Dead Band (mm)	Without disturbance	With disturbance
0	4.45	5.11
5	4.90	5.81
10	5.51	10.59

wave with different advantages and disadvantages. The rectangular wave, which has an abrupt change in pressure, excels when the pressure setpoints are also rectangular waves as demonstrated in the R-R mode. The abrupt change allows a faster change in pressure, leading to a faster response. Conversely, the abrupt change in pressure means that the time window that the valve needs to operate is very short when the setpoints are continuous waveforms. The delayed response of the valves led to a larger error in R-S mode as shown in Fig. 18.

In contrast, a sinusoidal source pressure has a gradual change in pressure, giving more time for the valves to operate. This results in a lower error than rectangular source pressure with a sinusoidal setpoint as shown in the S-S mode. However, a gradual pressure change also results in a slower response when a faster response is required, as shown in the S-R mode. Lastly, increasing the frequency in Sinusoidal mode shortens the time window for the valves and negates its advantage. This results in an error similar to that of the rectangular source pressure mode as shown in Fig. 20. A suitable configuration is required for the APCS to operate optimally, namely a rectangular source pressure for a step reference signal, and sinusoidal source pressure for a continuous reference signal.

In the position control mode, the APCS is designed to operate with single-acting cylinders as actuators. In this paper, we utilized double-acting cylinders as single-acting cylinders by supplying a constant air pressure on one side instead of a return spring which is more commonly used. However, we believe that a single-acting cylinder with a return spring as the return mechanism can also be used to a similar effect.

The specific experiment setup used in this paper cannot hold an overrunning load beyond the pneumatic pressure due to the limitations of a single-acting hydraulic cylinder. If the load is mainly in the extension direction, switching the pneumatic and hydraulic port will allow the load to be held. If both resistive load and overrunning load are required, changing the actuator to a double-acting cylinder with a 4/3 directional control valve will allow load in both directions to be help at the cost of a more complex valve and piping.

The challenges of implementation of APCS on the hardware are the limitations of the pump and operating speed of the valve which limit the maximum source frequency resulting in a larger error and slower response. With a faster valve, both faster response and lower error can be achieved. Another issue that was present on real hardware was valve leakage. This was solved by connecting two solenoid valves in an opposite direction. The computational complexity of the proposed controller is $O(n)$, where n is the number of actuators.

The main limitation of this study is that both the pressure and position are updated at semi-regular intervals instead of continuously. This may make APCS not suitable for certain applications where a smooth motion, a high-frequency oscillating setpoint, or an instantaneous response is required. However, APCS may be able to reduce power consumption and part complexity for multi-degree-of-freedom systems where a slower response is acceptable such as a jack-up system for structural adjustment and construction in civil engineering [19,20], or positioning of caisson foundation [21]. With faster equipment, the APCS will be able to provide a faster response and may be able to be adopted in mobile robots.

6. Conclusions

In this study, we developed the APCS based on an alternating supply system with feedback and a dynamic duty ratio. This system allowed the pressure and volume in each individual actuator to be controlled simultaneously and independently, and required only one centralized pump, and one on–off valve and feedback sensor for each actuator. Furthermore, we proposed a dynamic duty ratio equation that improves the energy usage in the pressure control mode and balances the performance of all actuators in the position control mode.

We simulated the system and found that in the pressure control mode, a rectangular wave source pressure is preferred for a rectangular wave setpoint while a sinusoidal wave source pressure is preferred for the sinusoidal wave setpoint. In addition, we also confirmed that the application of the dynamic duty ratio reduced the pump utilization time from 50% to 41.22% in the R-R mode. Further, in the position control mode, the system could follow the position command of each actuator independently, and increasing the alternating source pressure frequency reduced the delay and error in all operation modes.

The experimental results were consistent with the simulated results. We could operate four hydraulic cylinders in parallel with a similar error, which were delayed compared to the simulations. In the S-S mode, increasing the source frequency reduced the delay and increased the error, whereas both delay and error are reduced in the simulations. In the R-R mode with dynamic duty ratio, increasing the source pressure frequency reduces pump utilization to 21.96% at 3 Hz. Increasing the source frequency beyond 3 Hz produced a negligible change in pump utilization. In contrast, in the position control mode, increasing the alternating source frequency or dead band gap did not show a reduced error, but reduced the pump utilization considerably from 57.66% to 26.07%. The proposed system was able to operate under a loaded condition in both pressure control mode and position control mode, although with an increased error.

Future directions include conducting experiments in other load conditions, improving the algorithm to operate in an open-looped fashion with an implementation of an observer such as those proposed in [22], and the application of the system on a real robot.

CRediT authorship contribution statement

Sarin Kittisares: Conceptualization, Methodology, Software, Investigation, Writing – original draft. **Yosiharu Hirota:** Resources. **Hiroyuki Nabae:** Conceptualization, Methodology, Writing – review. **Gen Endo:** Conceptualization. **Koichi Suzumori:** Conceptualization, Methodology, Writing – review & editing, Supervision.

Declaration of competing interest

The authors declare that they have no known competing financial interests or personal relationships that could have appeared to influence the work reported in this paper.

Funding

This work was supported by the JSPS KAKENHI Grant-in-Aid for Scientific Research(A) grant number JP18H03760.

References

[1] Zang X, Liu Y, Zhu Y. Structure design of a mobile jack robot. In: 2013 IEEE international conference on information and automation. 2013, p. 1218–23. http://dx.doi.org/10.1109/ICINFA.2013.6720480.

[2] Kaminaga H, Ko T, Masumura R, Komagata M, Sato S, Yorita S, et al. Mechanism and control of whole-body electro-hydrostatic actuator driven humanoid robot hydra. In: Springer proceedings in advanced robotics, vol. 1, 2016, p. 656–65. http://dx.doi.org/10.1007/978-3-319-50115-4_57.

[3] Suzumori K, Faudzi AA. Trends in hydraulic actuators and components in legged and tough robots: a review. Adv Robot 2018;32(9):458–76. http://dx.doi.org/10.1080/01691864.2018.1455606.

[4] Hemmi M, Morita R, Hirota Y, Inoue K, Nabae H, Endo G, et al. Development of hydraulic tough motors with high power density and their application to a 7-axis robotic arm. In: Proceedings of the 2019 IEEE/SICE international symposium on system integration, SII 2019. Institute of Electrical and Electronics Engineers Inc. 2019, p. 264–9. http://dx.doi.org/10.1109/SII.2019.8700419.

[5] Raibert M, Blankespoor K, Nelson G, Playter R. Bigdog, the rough-terrain quadruped robot. IFAC Proc Vol 2008;41(2):10822–5. http://dx.doi.org/10.3182/20080706-5-KR-1001.01833.

[6] Semini C, Tsagarakis NG, Guglielmino E, Focchi M, Cannella F, Caldwell DG. Design of HyQ – a hydraulically and electrically actuated quadruped robot. Vol. 225. No. 6. 2011, p. 831–49. http://dx.doi.org/10.1177/0959651811402275.

[7] Kohlbrecher S, Romay A, Stumpf A, Gupta A, von Stryk O, Bacim F, et al. Human–robot teaming for rescue missions: Team vigir's approach to the 2013 DARPA robotics challenge trials. J Field Robotics 2015;32(3):352–77. http://dx.doi.org/10.1002/rob.21558.

[8] Li X, Zhou H, Feng H, Zhang S, Fu Y. Design and experiments of a novel hydraulic wheel-legged robot (WLR). In: IEEE international conference on intelligent robots and systems. 2018, p. 3292–7. http://dx.doi.org/10.1109/IROS.2018.8594484.

[9] Kaminaga H, Amari T, Niwa Y, Nakamura Y. Electro-hydrostatic actuators with series dissipative property and their application to power assist devices. In: 2010 3rd IEEE RAS and EMBS international conference on biomedical robotics and biomechatronics, BioRob 2010. 2010, p. 76–81. http://dx.doi.org/10.1109/BIOROB.2010.5626341.

[10] Song B, Lee D, Park SY, Baek YS. Design and performance of nonlinear control for an electro-hydraulic actuator considering a wearable robot. In: Processes 2019. Vol. 7. p. 389. http://dx.doi.org/10.3390/PR7060389, 7 (6) (2019) 389.

[11] Kittisares S, Nabae H, Endo G, Suzumori K, Sakurai R. Design of knee support device based on four-bar linkage and hydraulic artificial muscle. ROBOMECH J 2020;7(1). http://dx.doi.org/10.1186/s40648-020-00165-2.

[12] Alle N, Hiremath SS, Makaram S, Subramaniam K, Talukdar A. Review on electro hydrostatic actuator for flight control. Int J Fluid Power 2016;17(2):125–45. http://dx.doi.org/10.1080/14399776.2016.1169743.

[13] Chao Q, Zhang J, Xu B, Huang H, Pan M. A review of high-speed electro-hydrostatic actuator pumps in aerospace applications: Challenges and solutions. Trans ASME, J Mech Des 141(5). http://dx.doi.org/10.1115/1.4041582, (may 2019).

[14] Karanovic V, Jocanovic M, Jovanovic V. Review of development stages in the conceptual design of an electro hydrostatic actuator for robotics. Acta Polytechnica Hungarica 2014;11(5):59–79.

[15] Miyoshi T, Yoshida K, Eom SI, Yokota S. Proposal of a multiple ER microactuator system using an alternating pressure source. Sensors Actuators A 2015;222:167–75. http://dx.doi.org/10.1016/J.SNA.2014.12.002.

[16] Sudhawiyangkul T, Yoshida K, Eom SI, wan Kim J. A novel bending microactuator with integrated flexible electro-rheological microvalves using an alternating pressure source for multi-actuator systems. Microsyst Technol 2020;26(5):1507–19. http://dx.doi.org/10.1007/s00542-019-04685-9.

[17] Takahashi T, Yamashina C, Miyakawa S. Development of water hydraulic proportional control valve. In: Proceedings of the JFPS international symposium on fluid power 1999. No. 4. 1999, p. 549–54. http://dx.doi.org/10.5739/isfp.1999.549.

[18] Wang X, Yamaguchi A. Characteristics of hydrostatic bearing/seal parts for water hydraulic pumps and motors. Part 1: Experiment and theory. Tribol Int 2002;35(7):425–33. http://dx.doi.org/10.1016/S0301-679X(02)00023-3.

[19] Akai K, Tanaka Y. Ex-post-facto estimate of performance at the offshore reclamation of airport osaka/KIA. In: Proceedings of the 16th international conference on soil mechanics and geotechnical engineering. IOS Press; 2005, p. 1011–4. http://dx.doi.org/10.3233/978-1-61499-656-9-1011.

[20] Seo J, Yoo WS, Lee UK, Kim C, Kang KI, Cho H. Case study of a synchronous hydraulic jack-up system for constructing high-rise residential buildings. Can J Civil Eng 2010;37(6):922–6. http://dx.doi.org/10.1139/L10-026.

[21] Houlsby GT, Kelly RB, Huxtable J, Byrne BW. Field trials of suction caissons in sand for offshore wind turbine foundations. Geotechnique 2006;56(1):3–10. http://dx.doi.org/10.1680/geot.2006.56.1.3.

[22] Razmjooei H, Shafiei MH, Palli G, Ibeas A. Chattering-free robust finite-time output feedback control scheme for a class of uncertain non-linear systems. IET Control Theory Appl 2020;14(19):3168–78. http://dx.doi.org/10.1049/iet-cta.2020.0910.

Sarin Kittisares received his B.E. degree in Mechatronics from King Mongkut's University of Technology Thonburi, Bangkok, Thailand in 2017. He received the M.E. degree in Mechanical Engineering from Tokyo Institute of Technology, Tokyo, Japan in 2020, where he is currently pursuing his doctoral degree.

Yosiharu Hirota received his bachelor degree from the Department of Science and Engineering, Waseda University, Tokyo, Japan in 1968. From 1968, he worked for Yuken Kogyo Co. Ltd. In 2015, he joined the school of Engineering, Tokyo Institute of Technology as a researcher. He is a member of The Japan Fluid Power System Society.

Hiroyuki Nabae received his B.E., M.E., and Ph.D. degrees from the University of Tokyo, Tokyo, Japan in 2010, 2012, and 2015, respectively. He worked as a JSPS research fellow from April 2013 to March 2015. He is currently an assistant professor at Tokyo Institute of Technology. His research interests include mechatronics, robotics, and actuators.

Gen Endo received his B.E., M.E., and Ph.D. degree from Tokyo Institute of Technology, Japan in 1996, 1998, and 2000, respectively. From 2000 to 2007, he worked for Sony Corp. and was also a visiting researcher as the Advanced Telecommunication Research Institute International. In 2008, he joined the faculty of Tokyo Institute of Technology, as an assistant professor. In 2014, he was an associate professor of Institute of Biomaterials and Bioengineering in Tokyo Medical and Dental University. He is currently a professor of Tokyo Institute of technology. He is a member of the Japan Society of Mechanical Engineers, the Robotics Society of Japan, IEEE and The Society of Instrument and Control Engineers.

Koichi Suzumori was born in 1959. He received the BS, MS, and Ph.D. degrees in Mechanical Engineering from Yokohama National University, Japan, in 1982, 1984, and 1990, respectively. He had worked for Toshiba R&D Center from 1984 to 2001, and also worked for Micromachine Center, Tokyo, from 1999 to 2001. He had been a Professor of Division of Industrial Innovation Sciences, Okayama University, Japan since 2001. He has been a Professor of Department of Mechanical and Aerospace Engineering, Tokyo Institute of Technology since 2014. He is mainly engaging in the research fields of new actuators and their applications. He received many awards such as JSME Medal for Outstanding Paper, in 1999, RSJ Best Paper Award in 2000, and JSAEM Best Book Award in 2006. He is a fellow member of the Japan Society of Mechanical Engineers.